Schizophrenia Bulletin
doi:10.1093/schbul/sby046

Shared and Distinct Functional Architectures of Brain Networks Across Psychiatric Disorders

Mingrui Xia[1–3], Fay Y. Womer[4], Miao Chang[5,6], Yue Zhu[6,7], Qian Zhou[6,7], Elliot Kale Edmiston[6], Xiaowei Jiang[5,6], Shengnan Wei[5,6], Jia Duan[6,7], Ke Xu[5], Yanqing Tang[6,7], Yong He[1–3], and Fei Wang*[,5–7]

[1]National Key Laboratory of Cognitive Neuroscience and Learning, Beijing Normal University, Beijing, PR China; [2]Beijing Key Laboratory of Brain Imaging and Connectomics, Beijing Normal University, Beijing, PR China; [3]IDG/McGovern Institute for Brain Research, Beijing Normal University, Beijing, PR China; [4]Department of Psychiatry, Washington University School of Medicine, St. Louis, MO; [5]Department of Radiology, The First Affiliated Hospital of China Medical University, Shenyang, Liaoning, PR China; [6]Brain Function Research Section, The First Affiliated Hospital of China Medical University, Shenyang, Liaoning, PR China; [7]Department of Psychiatry, The First Affiliated Hospital of China Medical University, Shenyang, Liaoning, PR China

*To whom correspondence should be addressed; Department of Psychiatry and Radiology, The First Affiliated Hospital, China Medical University, 155 Nanjing North Street, Shenyang 110001, Liaoning, PR China; tel/fax: 8624-83283405, e-mail: fei.wang@cmu.edu.cn

Brain network alterations have increasingly been implicated in schizophrenia (SCZ), bipolar disorder (BD), and major depressive disorder (MDD). However, little is known about the similarities and differences in functional brain networks among patients with SCZ, BD, and MDD. A total of 512 participants (121 with SCZ, 100 with BD, 108 with MDD, and 183 healthy controls, matched for age and sex) completed resting-state functional magnetic resonance imaging at a single site. Four global measures (the clustering coefficient, the characteristic shortest path length, the normalized clustering coefficient, and the normalized characteristic path length) were computed at a voxel level to quantify segregated and integrated configurations. Interregional functional associations were examined based on the Euclidean distance between regions. Distance strength maps were used to localize regions with altered distances based on functional connectivity. Patient groups exhibited shifts in their network architectures toward randomized configurations, with SCZ>BD>MDD in the degree of randomization. Patient groups displayed significantly decreased short-range connectivity and increased medium-/long-range connectivity. Decreases in short-range connectivity were similar across the SZ, BD, and MDD groups and were primarily distributed in the primary sensory and association cortices and the thalamus. Increases in medium-/long-range connectivity were differentially localized within the prefrontal cortices among the patient groups. We highlight shared and distinct connectivity features in functional brain networks among patients with SCZ, BD, and MDD, which expands our understanding of the common and distinct pathophysiological mechanisms and provides crucial insights into neuroimaging-based methods for the early diagnosis of and interventions for psychiatric disorders.

Key words: connectome/functional connectivity/big data/high-resolution network/frontal cortex

Introduction

Increasingly, schizophrenia (SCZ), bipolar disorder (BD), and major depressive disorder (MDD) are conceptualized as brain network disorders.[1,2] Recent large-scale connectome studies have reported various topological alterations in the functional brain networks of patients with SCZ, BD, and MDD. These findings suggest subtle randomization within the brain network topology in patients with each of the 3 disorders and the loss of an optimal balance between segregated and integrated information processing.[3–5]

The topology of complex networks embedded within a physical space has recently become a significant area of focus, as it may further elucidate patterns of network organization among patients with SCZ, BD, and MDD. Specifically, measures of physical distance-dependent connectivity may reflect degrees of segregation, or specialized processing within interconnected brain regions, and integration, or the network capacity for rapid the combination of specialized information from distributed brain regions.[6] Recently, distance-dependent alterations in functional connectivity have been observed in patients with SCZ,[7,8] BD,[9] and MDD.[10] Similarities in the brain network are not surprising, as SCZ, BD, and MDD share common genetic and environmental risk factors,[11] potential neural mechanisms and alterations,[12] and clinical symptoms (eg, nonspecific or secondary symptoms involving sensory processing, sleep, appetite, motor coordination, and sequencing).[13] Further studies are needed

to determine the extent of the similarities and differences in functional brain networks among patients with SCZ, BD, and MDD. However, we are not aware of any published studies examining this topic.

Dynamic neurodevelopmental processes have significant influences on network characteristics.[14] These processes appear to depend on the range of distances between neural connections and the neurotransmitter milieu. As children mature into adults, local, short-range connections between adjacent brain regions shift to a greater proportion of long-range connections within the brain network.[15,16] The observed shift likely reflects the balance between synaptic pruning and the growth of length-dependent neuronal connections.[17,18] Neurotransmitters appear to determine the selectivity of synaptic pruning and preservation during development.[14,19] Interestingly, glutamine may direct short-range connections within subcortical regions including the thalamus, whereas GABA or GABA–dopamine interactions may shape long-range connections in the frontal lobe.[14] The resulting normative brain architecture is characterized by (1) high clustering with predominant short-range connections within the primary sensory and motor cortical areas and subcortical regions such as the thalamus and striatum, and (2) short average path lengths (high efficiency) with predominantly long-range connections in heteromodal cortices.[20]

Using a voxel-based graph analysis of a resting-state functional MRI (R-fMRI), in this study, we examined (1) global network properties, (2) whole-brain functional connectivity based on connectivity distances, and (3) distance strength maps to identify alterations in the functional brain networks among patients with SCZ, BD, and MDD. A voxel-wise approach avoids parcellation-dependent effects on the topological organization of brain networks.[21] We hypothesized the presence of randomization in the network configuration and distance-dependent alterations in functional connectivity among patients with SCZ, BD, and MDD.

Materials and Methods

Participants

Five hundred and fifty individuals (ages 13–45 years) participated in this study, including 139 with SCZ, 108 with BD, 114 with MDD, and 189 healthy controls (HCs). All participants provided written informed consent after receiving a detailed description of the study. The study was approved by the Institutional Review Board of China Medical University. All participants with SCZ, BD, and MDD were recruited from the inpatient and outpatient services at the Shenyang Mental Health Center and the Department of Psychiatry, First Affiliated Hospital of China Medical University, Shenyang, China. HC participants were recruited from the local community by advertisement. Two trained psychiatrists determined the presence or absence of Axis I psychiatric diagnoses in participants 18 years and older using the Structured Clinical Interview for Diagnostic and Statistical Manual of Mental Disorders, Fourth Edition (DSM-IV) Axis I Disorders and in participants younger than 18 years using the Schedule for Affective Disorders and Schizophrenia for School-Age Children-present and Lifetime Version (K-SADS-PL). Participants with SCZ, BD, or MDD met the DSM-IV diagnostic criteria for SCZ, BD, or MDD, respectively, and no other Axis I disorders. HC participants did not have a current or lifetime history of an Axis I disorder or a history of psychotic, mood, or other Axis I disorders in first-degree relatives, as determined from a detailed family history. Participants were excluded for (1) lifetime substance/alcohol abuse or dependence, (2) the presence of a concomitant major medical disorder, (3) any MRI contraindications, (4) a history of head trauma with loss of consciousness ≥5 minutes or any neurological disorder, and (5) suboptimal imaging data quality (see below for details). Symptoms and cognitive measures were obtained using the Brief Psychiatric Rating Scale (BPRS), Hamilton Depression Rating Scale (HAMD), Hamilton Anxiety Rating Scale (HAMA) and Young Mania Rating Scale (YMRS), and Wisconsin Card Sorting Test (WCST). Detailed demographic and clinical data are presented in table 1. This dataset will be shared with the academic community under limited open access guidelines in the future.

MRI Acquisition

MRI data were acquired using a GE Signa HD 3.0-T scanner (General Electric, Milwaukee, WI) with a standard 8-channel head coil at the First Affiliated Hospital of China Medical University, Shenyang, PR China. Functional images were collected using a gradient-echo planar imaging (EPI-GRE) sequence. The following parameters were used: TR = 2000 ms, TE = 30 ms, flip angle = 90°, field of view = 240 × 240 mm^2, and matrix = 64 × 64. Thirty-five axial slices were collected with a 3-mm thickness, without a gap. The scan lasted 6 minutes and 40 seconds, resulting in 200 volumes. Participants were instructed to rest and relax with their eyes closed but to remain awake during scanning. According to the responses to a simple questionnaire after the scan, none of the subjects had fallen asleep.

Data Preprocessing

All R-fMRI images were preprocessed using SPM12 (www.fil.ion.ucl.ac.uk/spm/) and DPARSF.[22] The first 10 time points were discarded for magnetic field stabilization and to allow participants to adapt to the scanning environment. The subsequent preprocessing steps included slice time correction and head motion correction. During head motion correction, 38 subjects (18 with SCZ, 8 with BD, 6 with MDD, and 6 HCs) were excluded from subsequent analyses due to excessive head motion, based on a criterion of 3 mm or 3°. (We also applied criteria of 2 mm/2°, 1 mm/1°, and mean frame-wise displacement of

Table 1. Demographics, Clinical Characteristics, and Cognitive Function of Healthy Controls and Patients With SCZ, BD, and MDD

	HC	SCZ	BD	MDD			
	(*n* = 183)	(*n* = 121)	(*n* = 100)	(*n* = 108)	Numerical Values	F/χ^2 Values	*P* Values
Demographic characteristics							
Age at scan, years	26.62 (8.00)	24.74 (9.03)	25.81 (8.31)	25.62 (8.43)	13–45	1.260	.287
Male	73 (40%)	54 (45%)	48 (48%)	35 (32%)		6.073	.108
Right-handed[a]	171 (96%)	100 (89%)	95 (97%)	93 (94%)		9.365	.154
Smoking status, yes[a]	30 (19%)	12 (14%)	21 (26%)	22 (24%)		4.474	.215
Clinical characteristics							
Duration, months	—	21.87 (36.15)	41.48 (56.18)	20.58 (31.00)	0.2–276	7.23	.001
First episode, yes[a]	—	86 (74%)	52 (57%)	85 (88%)		34.783	<.001
Medication, yes[a]	—	71 (59%)	65 (65%)	43 (40%)		172.356	<.001
Antidepressants[a]	—	4 (4%)	28 (29%)	35 (36%)		32.684	<.001
Antipsychotics[a]	—	59 (61%)	35 (36%)	1(1%)		78.535	<.001
Mood stabilizer[a]	—	4 (4%)	52 (53%)	0		116.526	<.001
HAMD-17	(*n* = 161)	(*n* = 86)	(*n* = 97)	(*n* = 106)			
	1.17 (1.70)	8.12 (6.96)	11.63 (9.52)	21.26 (8.75)	0–39	184.586	<.001
HAMA	(*n* = 162)	(*n* = 69)	(*n* = 96)	(*n* = 93)			
	0.86 (1.82)	6.80 (7.26)	8.52 (8.80)	16.32 (9.49)	0–42	100.105	<.001
YMRS	(*n* = 157)	(*n* = 60)	(*n* = 95)	(*n* = 89)			
	0.22 (.92)	2.20 (4.50)	8.07 (10.05)	1.47 (2.87)	0–36	43.721	<.001
BPRS	(*n* = 101)	(*n* = 116)	(*n* = 60)	(*n* = 45)			
	18.31(.82)	36.11 (14.00)	25.68 (8.43)	25.53 (6.21)	18–95	63.302	<.001
Cognitive function							
WCST	(*n* = 110)	(*n* = 58)	(*n* = 58)	(*n* = 66)			
Correct responses	29.13 (12.66)	18.14 (11.78)	23.47 (12.31)	23.27 (11.91)	0–48	10.797	<.001
Categories completed	3.81 (2.28)	1.57 (1.80)	2.69 (2.07)	2.83 (2.04)	0–8	14.93	<.001
Total errors	19.06 (12.74)	29.86 (11.78)	24.02 (12.41)	24.80 (11.91)	0–48	10.24	<.001
Perseverative errors	7.36 (7.92)	13.36 (12.52)	10.03 (10.28)	10.83 (9.60)	0–45	5.048	.002
Non-perseverative errors	11.56 (7.08)	16.50 (8.80)	14.36 (7.72)	13.97 (6.53)	0–33	5.925	.001
Head motion parameters							
Max translation, mm	0.56 (0.39)	0.67 (0.49)	0.66 (0.47)	0.68 (0.58)	0.09–2.74	1.893	.130
Max rotation, degree	0.55 (0.42)	0.64 (0.51)	0.61 (0.44)	0.66 (0.58)	0.07–2.83	1.636	.180
Mean FD, mm	0.11 (0.05)	0.12 (0.08)	0.12 (0.06)	0.11 (0.06)	0.04–0.59	2.124	.096

Note: Data are presented as either *n* (%) or means (standard deviations).
SCZ, schizophrenia; BD, bipolar disorder; MDD, major depressive disorder; HC, healthy control; WCST, Wisconsin Card Sorting Test; HAMD, Hamilton Depression Scale; HAMA, Hamilton Anxiety Scale; YMRS, Young Mania Rating Scale; BPRS, Brief Psychiatric Rating Scale.
[a]Information was missing for some participants.

0.2 mm for validation. The main results were consistent with our findings. See the supplementary materials for details.). No significant differences in head motion parameters were observed among the groups (all $P > .096$). Next, the corrected functional images were normalized to the MNI space using the EPI template in SPM12, resampled to 3-mm isotropic voxels, and further smoothed via a Gaussian kernel with a 4-mm full-width at half-maximum. Linear detrending was performed and several confounding covariates, including the Friston-24 head motion parameters, white matter, cerebrospinal fluid, and global signals, were regressed from the BOLD time series for all voxels. Finally, temporal band-pass filtering (0.01–0.1 Hz) was applied to the regressed fMRI data.

Network Construction

The construction of individual functional networks was constrained within a gray matter (GM) mask of 45,381 voxels, which was generated by extracting overlapping voxels in the automated anatomical labeling template[23] and the thresholded prior GM probability map (>0.2) provided by SPM12. We computed Pearson's correlation coefficients between all pairs of nodes (ie, GM voxels), resulting in 45,381 × 45,381 correlation matrices for each subject. These individual correlation matrices were further binarized with a density threshold of 1%, corresponding to the remaining 10,296,948 edges with top positive strength. Notably, 2 other densities of 0.5% and 2% were also used for validation analysis.

Global Network Measurements

To investigate the global network architectures, we calculated 4 network measurements for each subject: the clustering coefficient (*Cp*), the characteristic shortest path length (*Lp*), the normalized clustering coefficient (γ, ie, Cp/Cp_{rand}), and the normalized characteristic path length

(λ, ie, Lp/Lp_{rand}).[24] Specifically, Cp_{rand} and Lp_{rand} refer to the average Cp and Lp values obtained from 10 surrogate random networks, respectively. The surrogate random network was generated with the same numbers of nodes and edges and an identical degree distribution as the original brain networks. Notably, Cp and Cp_{rand} quantify the functional segregation and Lp and Lp_{rand} quantify the functional integration of brain networks.[24,25] See the supplementary materials for the detailed formula. The network construction and calculations of global network measurements were performed using the PAGANI toolkit (https://www.nitrc.org/projects/pagani_toolkit/),[26] which was developed based on our previously established CPU-GPU hybrid framework[27] to facilitate the rapid calculation of high-resolution voxel-based brain networks. This toolbox has been used to investigate the test-retest (TRT) reliability of graph metrics of voxel-based functional brain networks.[28]

Distance-Dependent Distribution of Network Connections

Network topologies are strongly associated with the connectivity distance (ie, Euclidean distance) between regions.[29] We calculated the Euclidean distance d_{ij} as an approximate anatomical distance of functional connectivity between voxel i and voxel j. Next, we divided whole-brain functional connectivity into 18 bins, with Euclidean distances binned into 10-mm steps ranging from 0 to 180 mm (the longest distance between voxels in the GM mask). Finally, we counted the number of edges within each distance bin for each subject and compared the values among groups.

Regional Distance Strength

Adjacent distance bins were combined if significant differences were observed in the group analysis and similar patterns of alterations in the patient groups were observed compared with HCs to minimize the use of multiple comparisons and reduce the chance of type I error. For example, significant differences were observed for distance bins 1 (0–10 mm) and 2 (10–20 mm), which were combined to create a distance bin of 0–20 mm. For each combined distance bin, we calculated the distance strength for each node to further examine specific regions displaying altered distance-dependent network connectivity. The distance strength of a given node was calculated as the total length of the edges linking to this node within the connectivity distance range, which captures both the number of connections and the approximate physical cost. Individual distance strength maps were generated for each distance bin and were compared across groups in a voxel-wise fashion.

Statistical Analyses

Group effects on clinical variables, global network measurements, connections in distance bins, and distance strength maps were examined using 1-way analysis of covariance (ANCOVA), with age and gender as covariates. Post hoc pair-wise analyses were performed using a general linear model for significant group effects in the ANCOVA. Significance for analyses of demographic and clinical characteristics, and global network measurements was set to $P < .05$. For analyses involving multiple distance bins, the false discovery rate (FDR) correction was applied for multiple comparisons, and significance was set to a corrected $P < .05$. An additional, more conservative Bonferroni-corrected $P < .05$ was also utilized to identify the most significant results. Analyses of distance strength maps were performed in a voxel-wise manner and significance was set to a voxel-level inference of $P < .001$, with a Gaussian random field correction for cluster-level inference of $P < .05$.

Analyses were also performed to examine relationships between the clinical and cognitive variables and global network measurements (ie, Cp, Lp, γ, and λ) and range-dependent strength in regions with significant between-group differences. See the supplementary materials for a detailed description.

Validation Analyses

We examined the influences of the clinical and demographic variables (ie, medication status, education level, and participants' ages) and of different network analyses and imaging preprocessing strategies (ie, network densities, local connections, global signal regression, signal-to-noise ratio of fMRI images, and head motion control) to validate our main findings. In particular, because age and head motion are 2 important factors in brain network analyses, we utilized different strategies to control their potential effects when analyzing the data (eg, strict criteria for selecting data and controlling for covariates in statistical models). Overall, our main conclusions were not influenced (for details, see the supplementary materials).

Results

Demographic and Clinical Data

No significant differences in age, sex, or handedness were observed among the SCZ, BD, MDD, and HC groups. However, significant differences were observed in illness duration, medication status, and first episode status, as well as HAMD, HAMA, YMRS, and BPRS total scores, among the SCZ, BD, and MDD groups (all $P < .05$).

Randomized Network Configurations in SCZ, BD, and MDD Groups

Significant group effects on all global network measurements (Cp, Lp, λ, and γ) were observed in the analyses of the 4 groups (all $P < .038$), with a descending order of HC, MDD, BD, and SCZ for mean values (figure 1). Post hoc

analyses revealed a significantly decreased *Cp* in the MDD, BD, and SCZ groups compared with HCs (all $P < .045$). *Lp* and λ were significantly decreased in the SCZ and BD groups compared with HCs (both $P < .025$), and γ was significantly decreased in the SCZ group compared with HCs ($P < .001$). These results suggest a shift toward a randomized network configuration in patients with SCZ, BD, and MDD, with SCZ>BD>MDD in the degree of randomization compared with HCs. Among the patient groups, the SCZ group displayed significantly decreased *Cp*, γ, and λ compared with the MDD group (all $P < .032$).

Altered Distance-Dependent Functional Connectivity in SCZ, BD, and MDD Groups

Significant group effects on distance bins 1 (0–10 mm), 2 (10–20 mm), 5 (40–50 mm), 6 (50–60 mm), 7 (60–70 mm), and 8 (70–80 mm) were observed (all $P < .014$, FDR-corrected, figure 2A and table S1). Post hoc comparisons between groups for each distance bin indicated an order of HC>MDD>BD>SCZ for the number of short-range connections (distance bins 1 [0–10 mm] and 2 [10–20 mm]) and, conversely, SCZ>BD>MDD>HC for the number of medium-/long-range connections (distance bins 5 [40–50 mm], 6 [50–60 mm], 7 [60–70 mm], and 8 [70–80 mm]). Compared with HCs, all 3 patient groups had significantly fewer short-range connections of 0–20 mm (distance bins 1 and 2) (all $P < .035$) and more medium-/long-range connections of 50–70 mm (distance bins 6 and 7) (all $P < .005$). Additionally, the SCZ and BD groups had significantly more medium-/long-range connections of 40–50 mm and 70–80 mm (distance bins 5 and 8) than the HC group, but significant differences in these distance bins were not observed between the MDD and HC groups. Among patient groups, the SCZ group displayed significantly fewer short-range connections but more medium-/long-range connections than the MDD group (all $P < .048$) (figure 2B). Significant differences in the other distance bins were not observed among the 4 groups (distance bins 3, 4, and 9–18). Notably, with the exception of bin 8, all these results remained significant at a level of $P < .05$ after the Bonferroni correction.

Distance Strength Patterns Among the SCZ, BD, and MDD Groups

Significant group differences in the distance strength of short-range connections (0–20 mm) were mainly localized in the primary visual, auditory, and association cortices, as well as the thalamus (figure 3A) with HC>MDD>BD>SCZ. Post hoc analysis revealed significantly lower short-range distance strength in patient groups than in HCs, with the exception of the primary and association motor/sensorimotor cortices in the MDD group (table 2). Significant group differences in the distance strength of medium-/long-range connections (40–80 mm) were primarily located in the prefrontal cortex (PFC), with significantly increased distance strength among the patient groups compared with HCs. Specifically, significant increases in distance strength were primarily observed in the bilateral dorsolateral prefrontal cortex (DLPFC) and left orbital frontal cortex (OFC) in the SCZ group, in the bilateral DLPFC in the BD group, and in the right DLPFC in the MDD group compared with HCs. Significantly increased distance strengths of medium-/long-range connections were also found in the left supplementary motor area (SMA) in the SCZ and BD groups compared with HCs (figure 3B and table 2). The extents of the medium-/long-range connections (40–80 mm) from the peaks of these regions are illustrated in figure S1.

Discussion

In this study, we observed (1) a shift toward a randomized configuration in the whole-brain network; (2) fewer short-range connections and more long-range connections; (3) decreases in the short-range distance strength involving the primary sensory and association cortices and thalamus and increases in the medium-/long-range distance strength with differential localization in the PFC among the SCZ, BD, and MDD groups; and (4) a gradient in the extent of alterations such that SCZ>BD>MDD. To our knowledge, this transdiagnostic study is the first to report voxel-wise functional brain network architectures

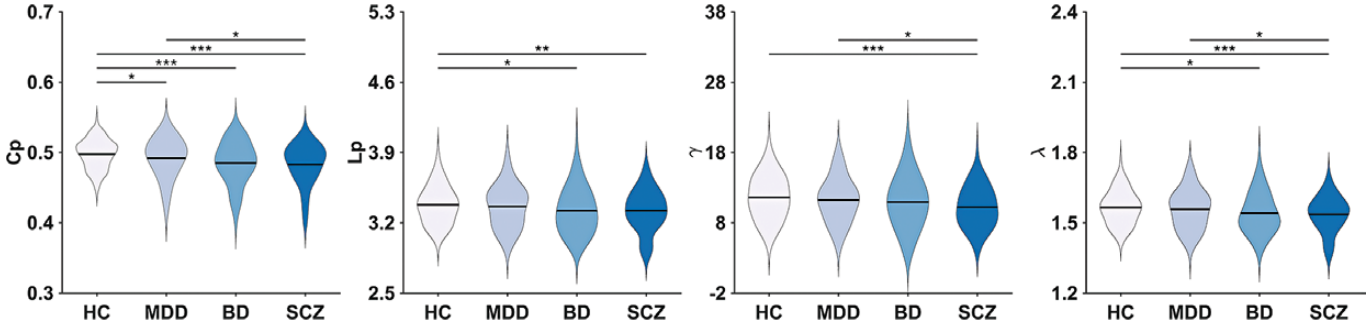

Fig. 1. Differences in global network parameters among the 4 groups. Violin plots represent the distribution of each global network parameter in each group and solid lines indicate the medians. The significance level was set to $P < .05$. *$P < .05$, **$P < .01$, ***$P < .001$. HC, healthy control; MDD, major depressive disorder; BD, bipolar disorder; SCZ, schizophrenia.

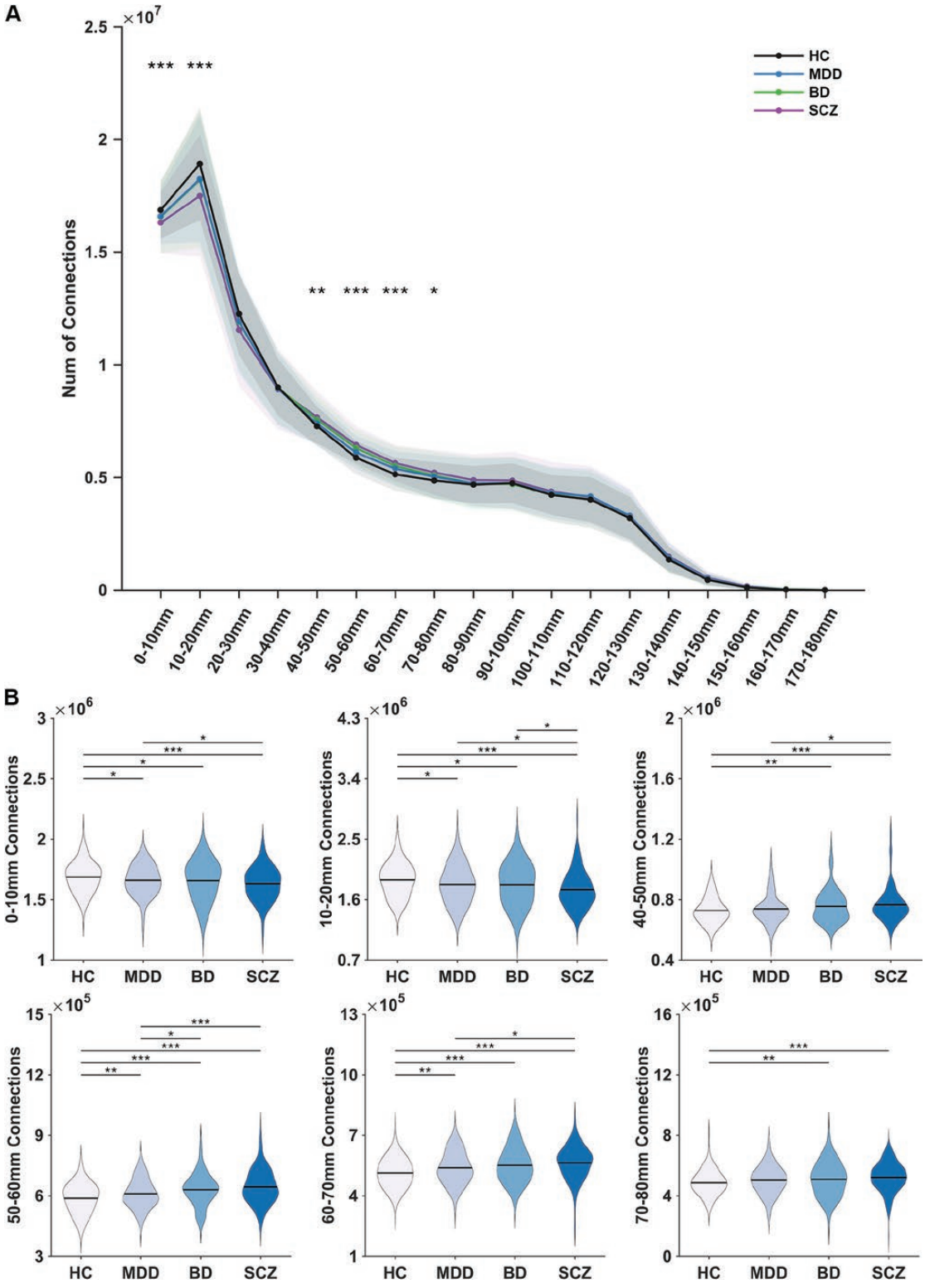

Fig. 2. Distance-dependent differences in the number of network connections among the 4 groups. (A) Group effects on the number of functional connections in each distance bin were detected by 1-way analysis of covariance. The solid line indicates the mean value for each group across distance bins and the shadow represents the standard deviation. (B) Between-group differences in bins 1, 2, 5, 6, 7, and 8 were further assessed using post hoc analyses. Violin plots represent the distribution of numbers of connections in each group and solid lines indicate medians. The significance level was set to $P < .05$, with an FDR correction for multiple comparisons. *$P < .05$, **$P < .01$, ***$P < .001$. HC, healthy control; MDD, major depressive disorder; BD, bipolar disorder; SCZ, schizophrenia.

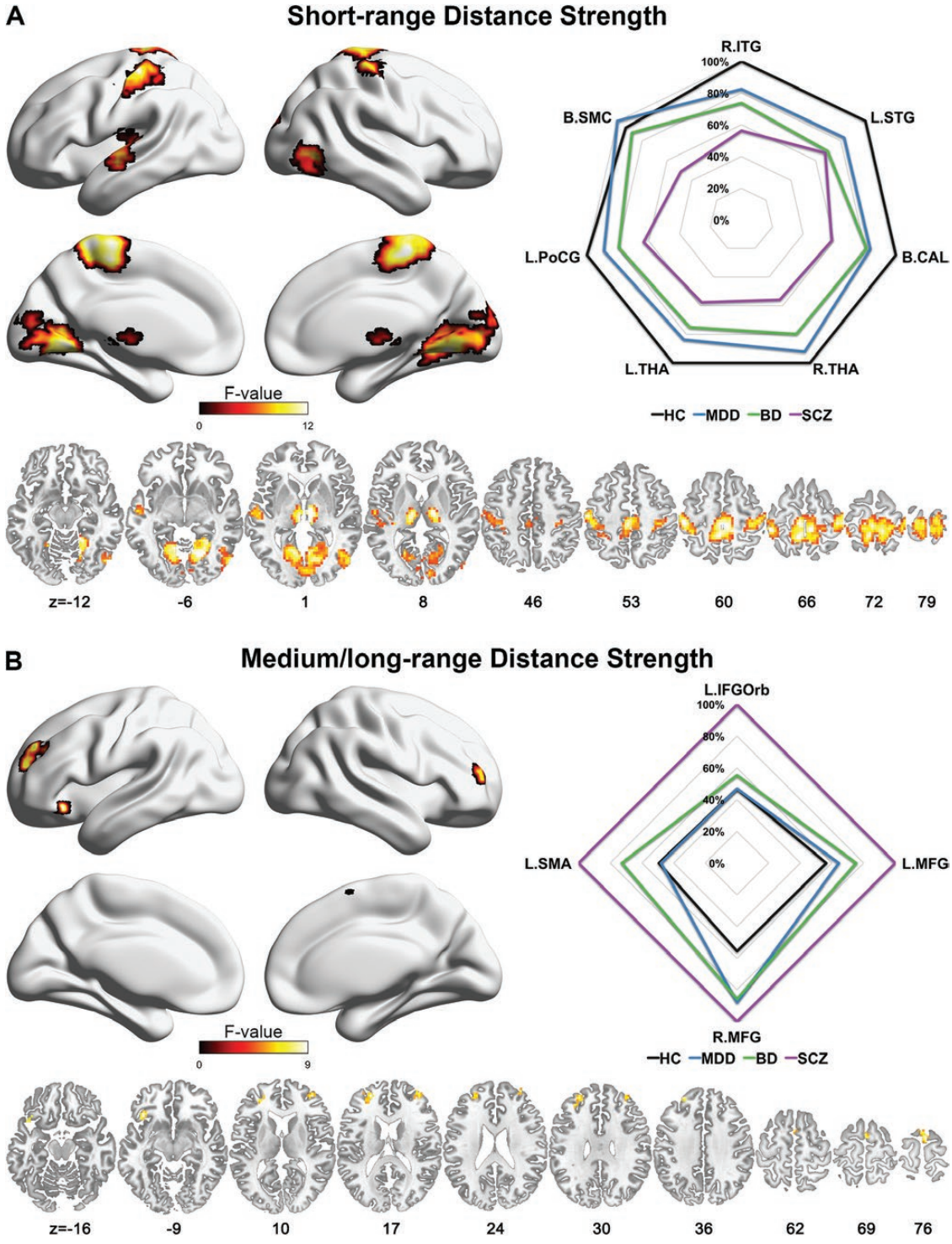

Fig. 3. Regions with significant group effects on short-range or medium-/long-range distance strength. (A) The 3-dimensional surface illustrates regions with significant group effects on short-range distance strength (0–20 mm). The radar plot shows the normalized mean values for each group at the peak of the significant cluster. For each peak, normalization was performed by dividing the mean values by the maximum mean value obtained from the 4 groups. (B) The 3-dimensional surface illustrates regions with significant group effects on medium-/long-range distance strength (40–80 mm). The radar map shows the normalized mean values for each group at the peak of the significant cluster. The significance level was set to $P < .001$ at the voxel level, with Gaussian random field corrections for multiple comparisons. HC, healthy control; MDD, major depressive disorder; BD, bipolar disorder; SCZ, schizophrenia; R, right; L, left; B, bilateral; ITG, inferior temporal gyrus; STG, superior temporal gyrus; CAL, calcarine; THA, thalamus; PoCG, postcentral gyrus; SMC, sensorimotor cortex; IFGOrb, inferior frontal gyrus, orbital part; MFG, middle frontal gyrus; SMA, supplementary motor area. The surface visualization was conducted by using BrainNet Viewer.[97]

Table 2. Regions Showing Abnormal Distance Strength

Distance	Region	Brodmann Areas	Cluster Size	Peak Coordinate			*F*-Value	*P*-Value	Post Hoc Analysis	η^2
Short-range connections	Right hemisphere Visual association cortex Inferior temporal gyrus	19/37	160	54	−72	−6	11.022	1.0×10^{-6}	MDD<HC, $P = .022$; BD<HC, $P = .002$; SCZ<HC, $P < .001$; SCZ<MDD, $P = .004$; SCZ<BD, $P = .044$	.061
	Left hemisphere Primary auditory cortex Superior temporal gyrus	22/41/42	140	−54	−21	3	10.331	1.0×10^{-6}	MDD<HC, $P = .016$; BD<HC, $P < .001$; SCZ<HC, $P < .001$; SCZ<MDD, $P = .034$	.058
	Bilateral Primary visual cortex Visual association cortex	17/18/19	862	21	−63	−6	13.914	$<1.0 \times 10^{-6}$	MDD<HC, $P = .012$; BD<HC, $P = .006$; SCZ<HC, $P < .001$; SCZ<MDD, $P = .001$; SCZ<BD, $P = .002$	.076
	Right hemisphere Thalamus	NA	143	15	−18	9	13.215	$<1.0 \times 10^{-6}$	BD<HC, $P = .011$; SCZ<HC, $P < .001$; SCZ<MDD, $P < .001$; SCZ<BD, $P = .003$	.073
	Left hemisphere Thalamus	NA	133	−12	−15	9	12.107	$<1.0 \times 10^{-6}$	MDD<HC, $P = .016$; BD<HC, $P = .002$; SCZ<HC, $P < .001$; SCZ<MDD, $P = .002$; SCZ<BD, $P = .025$	.067
	Left hemisphere Primary motor cortex Motor association cortex Primary somatosensory area Somatosensory association cortex	1/2/3/4	285	−45	−27	60	13.585	$<1.0 \times 10^{-6}$	BD<HC, $P = .001$; SCZ<HC, $P < .001$; SCZ<MDD, $P < .001$; SCZ<BD, $P = .015$	.075
	Bilateral Primary motor cortex Motor association cortex Primary somatosensory area Somatosensory association cortex	1/2/3/4/5/6	1076	−3	−42	60	14.188	$<1.0 \times 10^{-6}$	SCZ<HC, $P < .001$; SCZ<MDD, $P < .001$; SCZ<BD, $P < .001$	.078
Medium-/long-range connection	Left hemisphere Orbital frontal cortex	47	30	−39	24	−9	10.592	1.0×10^{-6}	HC<SCZ, $P < .001$; MDD<SCZ, $P < .001$; BD<SCZ, $P < .001$	.059
	Left hemisphere Dorsolateral prefrontal cortex	10	81	−27	48	33	9.057	8.0×10^{-6}	HC<BD, $P = .042$ HC<SCZ, $P < .001$; MDD<SCZ, $P < .001$; BD<SCZ, $P = .011$	.051

Table 2. *Continued*

Distance	Region	Brodmann Areas	Cluster Size	Peak Coordinate			*F*-Value	*P*-Value	Post Hoc Analysis	η^2
	Right hemisphere Dorsolateral prefrontal cortex	10	53	39	51	12	8.291	2.2×10^{-5}	HC<MDD, $P = .001$ HC<BD, $P = .004$; HC<SCZ, $P < .001$	.047
	Left hemisphere Supplementary motor area	6	34	0	−3	72	9.428	5.0×10^{-6}	HC<BD, $P = .039$ HC<SCZ, $P < .001$; MDD<SCZ, $P < .001$ BD<SCZ, $P = .022$	.053

Note: The significance level was set to $P < .05$ and a corrected $P < .001$ at the voxel level using Gaussian random field corrections for multiple comparisons.
HC, healthy control; MDD, major depressive disorder; BD, bipolar disorder; SCZ, schizophrenia.

among patients with SCZ, BD, and MDD. Prior studies have largely focused on comparisons of patients with an individual disorder with HCs. Our findings are largely consistent with previously observed network alterations in patients with SCZ,[4] BD,[30] and MDD.[3] Direct comparisons between 2 disorders have primarily identified significantly decreased network connections in limbic structures and increased network connections in frontal and parietal regions in both patients with SCZ and BD.[31,32] Furthermore, more widespread decreases in network connections involving sensory and subcortical regions have been observed in patients with SCZ.[32] According to a recent study utilizing R-fMRI data, both patients with SCZ and BD exhibit significantly reduced global efficiency in the cingulo-opercular network compared with HCs.[33] These findings implicate shared and distinct networks in patients with SCZ and BD.[31,34] Findings from comparisons between patients with BD and MDD have been inconsistent[35]; however, they suggest significant differences in functional networks at rest and during tasks between patients with BD and MDD.[36–38] Notably, an intriguing recent study used R-fMRI data to examine the relationship between reward responsivity and functional connectivity in patients with MDD, BD, and SCZ.[39] The authors revealed a common dysconnectivity pattern in the default mode and cingulo-opercular systems, providing further evidence of shared disturbances in functional brain networks in patients with psychiatric disorders.

The distance-dependent findings presented here are of particular interests. Shared decreases in short-range connections were observed in the primary sensory cortices and their association cortices and thalamus among patients with SZ, BD, and MDD, with differences in the localization of increased medium-/long-range connections within the PFC among patients with these disorders. These findings suggest a disrupted balance between network segregation and integration in patients with SCZ, BD, and MDD: diminished "segregation" of neural processing with weakening of short-range connections in the primary sensory and association cortices and thalamus and over-"integration" among distant regions via increased medium-/long-range connections in the PFC. These alterations may lead to inaccurate and inefficient information processing and synthesis within the brain network. Interestingly, a recent multimodal imaging study reported increased coupling between the structural and functional connectivity of long-distance connections in both the offspring of subjects with SCZ and the offspring of subjects with BD, consistent with our findings.[40] Specifically, altered sensory processing, which underlies the nonspecific or secondary symptoms observed among patients with SCZ, BD, and MDD, may provide inaccurate input to higher order regions, such as the PFC, and result in inappropriate or maladaptive learning and adaptation within neural circuits.[41] These maladaptations may then feed back into sensory processing circuits and create

a cycle for progressive and persistent disruptions within the functional brain network and lead to the clinical manifestations observed in patients with SCZ, BD, and MDD. Additionally, EEG studies have reported excessive low frequency (eg, delta band) activity in psychiatric disorders.[42,43] Given that carrier waves in the low-frequency spectrum are discussed for widespread connectivity and fast oscillations such as gamma are considered to be executed locally,[43] our findings in MRI data are somehow in line with the neurophysiological modality. Further studies are needed to confirm these hypotheses.

Differential localization of the increased medium-/long-range connections in the PFC was observed in this study: the bilateral DLPFC and OFC in patients with SCZ, the bilateral DLPFC in patients with BD, and the right DLPFC in patients with MDD. The PFC is a major site for cortico-cortical and thalamo-cortical integration and for the integration of multiple sensory modalities.[44] Recent large-scale network analyses support the critical importance of long-range connectivity in the PFC.[45] Alterations in dendritic spines in the PFC have been reported in subjects with SCZ, BD, and MDD,[46,47] and these changes likely contribute to the gain or loss of network connectivity.[48,49] Additionally, the motor/sensorimotor cortices or SMA may also serve as a differentiating marker. For example, the MDD group did not show alterations in short-range connections in the motor/sensorimotor and association cortices, or in medium-/long-range connections in the SMA, suggesting potential features that may differentiate MDD from other disorders. In addition, a gradient of network alterations appears among the disorders, with the extent of changes in the order of SCZ>BD>MDD, mirroring the clinical severity and outcomes for patients with these disorders.[50,51]

Previous studies have suggested a "hypofrontality" hypothesis that implicates deficits in PFC function in patients with SCZ, such as reduced glucose utilization and blood flow in the PFC during the resting state[52] and working memory tasks.[53,54] Meanwhile, a hypothesis of "inefficiency" in the PFC has also been proposed, suggesting that the compromised function of the PFC in patients with SCZ may result in either hyperfrontality or hypofrontality, depending on the cognitive task involved and the relative level of task demand.[55,56] Moreover, a clear and consistent conclusion regarding whether the PFC exhibits "hypofrontality" or "hyperfrontality" is still lacking, as evidence for both hypotheses has been presented.[57–59] For instance, both increased and decreased low-frequency spontaneous activity in the PFC has been reported in patients with SCZ in some R-fMRI studies, and the hyperactivity observed in patients with SCZ seemed to be more widespread to the superior/middle and inferior frontal gyri.[60–62] These variations might result from the limited statistical power of studies examining a small sample and from the large variations in the characteristics of recruited patients (eg, patients' race, cultural background, standard of diagnosis, and subtypes of patients) or research strategies utilized (eg, imaging protocols, preprocessing strategies, and measurement parameters) across studies.[2,63]

In contrast to local brain activity, functional connectivity measures the synchronization of activities between distant brain areas.[64] Previous studies have also reported hyperconnectivity of the PFC in patients with SCZ during the resting state.[65–67] Our results are consistent with these findings, and thus provide further evidence for "hyperfrontality" in the PFC of patients with SCZ. However, the neuronal mechanisms underlying the hypofrontality and hyperfrontality models remain unclear, and we speculate that either of the models may be associated with specific conditions. Future studies of a large sample with better homogeneity in the characteristics of the recruited patients and a more refined experimental design might provide researchers a crucial opportunity to understand the complexity of alterations in frontal activity in patients with SCZ.

Limitations and Further Considerations

Several issues warrant further consideration. First, we did not use intelligence tests to directly exclude patients with intellectual disabilities. Because individuals with intellectual disabilities may not progress further than their fourth year of elementary school,[68] we used the education level as an approximate measure of intelligence to exclude participants with a possible intellectual disability. The validation results were largely consistent with the main findings; however, the lack of a direct intelligence test is a limitation of this study and should be included in a future study. Moreover, there was a significant difference in education level among the 4 groups. Although our main conclusion remained stable after adding education level as an additional covariation in statistical analyses (for details, see the supplementary materials), this issue needs attention in future participant recruitments. Second, we did not monitor the participants' wakefulness during the R-fMRI scan. Although the investigators communicated with the participants before the beginning and immediately after the end of the R-fMRI scan, we were not completely convinced that all participants remained awake during the scan. Because neuroimaging studies have reported sleep-related connectivity changes in functional brain networks,[69–71] this issue deserves attention in task-free imaging studies. Recent advances in simultaneously recording physiological signals (eg, EEG) with fMRI will be helpful in resolving this issue. Third, human brain functional connectivity fluctuates over a range of temporal scales in coordination with internal states and environmental demands. However, the temporal resolution of R-fMRI is still relatively poor. Future studies combining fMRI and high temporal resolution electrophysiological recordings will provide researchers important opportunities to explore the neurophysiological

substrates that underlie the functional abnormalities in patients with psychiatric disorders.[72,73] Fourth, the abnormal functional connectivity architectures in patients with psychiatric disorders detected using R-fMRI are mainly obtained from a macroscale perspective, which is considered to partially reflect the distant communication of clustered neurons at the microscale.[74,75] Currently, the microscale brain networks are able to be constructed only within a local area due to technical limitations.[76,77] The gap between different scales still needs to be bridged with newly developed high-resolution imaging methods and validated biophysical models. Fifth, several studies have reported a significant association between functional and structural brain networks,[78–81] and some models have been constructed to predict the architectures of the functional networks based on anatomical constraints.[82–84] Both structural and functional abnormalities have been widely documented in patients with psychiatric disorders, and future studies linking the multimodal changes may further illustrate the interactions between brain alterations underlying symptoms of each disorder. Sixth, in this study, we observed neither significant group effects on head motion parameters nor significant correlations between these parameters and age ($P = .326$, $P = .249$, and $P = .201$ for the maximum translation, maximum rotation, and mean frame-wise displacement, respectively), suggesting that our findings were probably not driven by head motion. However, recent studies have suggested that head motion is not only a confounding factor that can influence estimates of functional brain connectivity,[85,86] but also a within-subject trait-like effect that correlates across scanning sessions,[86,87] with genetic[88,89] and neurobiological bases[87] and cognitive relevance.[90] The potential effects of head motion on functional networks among patients with different psychiatric disorders still need to be further investigated. Seventh, although we did not observe differences between un-medicated and medicated patients or between different medication types in any of the 3 patient groups, we cannot conclude that medications have no effects on functional connectome in psychiatric patients. Future study with longitudinal design could better deepen our understanding of the medication effects on the functional connectome in psychiatric disorders. Finally, the individual heterogeneity and subtyping of patients with these psychiatric disorders were not considered in this study. Recent studies demonstrated considerable variability in functional connectome between individuals,[91] which can act as fingerprint to identify individual from others.[92,93] Moreover, Drysdale et al.[94] offered a promising example for classifying patients with depression into different neurophysiological subtypes according to distinct patterns of dysfunctional connectivity. Investigations focusing on the convergent and divergent disconnects in brain networks in individual patients and subtypes of psychiatric disorders would certainly contribute to improving our understanding of the pathology of psychiatric disorders and the development of potential network biomarkers for early individual diagnosis.[95,96]

In summary, the organizational configurations of the whole-brain functional network exhibited a shift toward randomization among patients with SCZ, BD, and MDD. Furthermore, network alterations appear to depend on distance, with decreased short-range connectivity and increased medium-/long-range connectivity in patients with SCZ, BD, and MDD. Some aspects of these distance-dependent changes appear to be region specific and occur in a graded manner among patients with SCZ, BD, and MDD. Our findings enhance our understanding of the common and distinct pathophysiological mechanisms and provide crucial insights into neuroimaging-based methods for the early diagnosis of and interventions for psychiatric disorders.

Supplementary Material

Supplementary data are available at *Schizophrenia* Bulletin online.

Funding

This work was supported by National Natural Science Foundation of China (81671767 and 81401479 to M.X.; 81620108016 to Y.H.; 81571311, 81071099, and 81271499 to Y.T.; and 81571331 to F.W.); National Science Fund for Distinguished Young Scholars (81725005 to F.W.), Liaoning Education Foundation (Pandeng Scholar, F.W.) and Beijing Natural Science Foundation (Z161100004916027 and Z151100003915082 to Y.H. and Z161100000216125 to M.X.); National Key Research and Development Program (2016YFC0904300 to F.W.); National Key Research and Development Program (2016YFC1306900 to Y.T.); National High Tech Development Plan (863) (2015AA020513 to F.W.); and Fundamental Research Funds for the Central Universities (2017XTCX04 and 2015KJJCA13 to Y.H.).

Acknowledgment

We gratefully acknowledge the support of NVIDIA Corporation with the donation of the Tesla K40 GPU used for this research.
Conflict of interest: The authors declare no conflict of interest.

References

1. Fornito A, Zalesky A, Breakspear M. The connectomics of brain disorders. *Nat Rev Neurosci*. 2015;16:159–172.
2. Gong Q, He Y. Depression, neuroimaging and connectomics: a selective overview. *Biol Psychiatry*. 2015;77:223–235.
3. Zhang J, Wang J, Wu Q, et al. Disrupted brain connectivity networks in drug-naive, first-episode major depressive disorder. *Biol Psychiatry*. 2011;70:334–342.

4. Liu Y, Liang M, Zhou Y, et al. Disrupted small-world networks in schizophrenia. *Brain*. 2008;131:945–961.
5. Spielberg JM, Beall EB, Hulvershorn LA, Altinay M, Karne H, Anand A. Resting state brain network disturbances related to hypomania and depression in medication-free bipolar disorder. *Neuropsychopharmacology*. 2016;41:3016–3024.
6. Aerts H, Fias W, Caeyenberghs K, Marinazzo D. Brain networks under attack: robustness properties and the impact of lesions. *Brain*. 2016;139:3063–3083.
7. Alexander-Bloch AF, Vértes PE, Stidd R, et al. The anatomical distance of functional connections predicts brain network topology in health and schizophrenia. *Cereb Cortex*. 2013;23:127–138.
8. Lo CY, Su TW, Huang CC, et al. Randomization and resilience of brain functional networks as systems-level endophenotypes of schizophrenia. *Proc Natl Acad Sci USA*. 2015;112:9123–9128.
9. Özerdem A, Güntekin B, Atagün I, Turp B, Başar E. Reduced long distance gamma (28-48 Hz) coherence in euthymic patients with bipolar disorder. *J Affect Disord*. 2011;132:325–332.
10. Bohr IJ, Kenny E, Blamire A, et al. Resting-state functional connectivity in late-life depression: higher global connectivity and more long distance connections. *Front Psychiatry*. 2012;3:116.
11. Cross-Disorder Group of the Psychiatric Genomics C. Identification of risk loci with shared effects on five major psychiatric disorders: a genome-wide analysis. *Lancet*. 2013;381(9875):1371–1379.
12. Goodkind M, Eickhoff SB, Oathes DJ, et al. Identification of a common neurobiological substrate for mental illness. *JAMA Psychiatry*. 2015;72:305–315.
13. Levit-Binnun N, Davidovitch M, Golland Y. Sensory and motor secondary symptoms as indicators of brain vulnerability. *J Neurodev Disord*. 2013;5:26.
14. Ghisleni C, Bollmann S, Poil SS, et al. Subcortical glutamate mediates the reduction of short-range functional connectivity with age in a developmental cohort. *J Neurosci*. 2015;35:8433–8441.
15. Dosenbach NU, Nardos B, Cohen AL, et al. Prediction of individual brain maturity using fMRI. *Science*. 2010;329:1358–1361.
16. Fair DA, Dosenbach NU, Church JA, et al. Development of distinct control networks through segregation and integration. *Proc Natl Acad Sci USA*. 2007;104:13507–13512.
17. Biane JS, Scanziani M, Tuszynski MH, Conner JM. Motor cortex maturation is associated with reductions in recurrent connectivity among functional subpopulations and increases in intrinsic excitability. *J Neurosci*. 2015;35:4719–4728.
18. Toga AW, Thompson PM, Sowell ER. Mapping brain maturation. *Trends Neurosci*. 2006;29:148–159.
19. Bourgeois JP, Rakic P. Changes of synaptic density in the primary visual cortex of the macaque monkey from fetal to adult stage. *J Neurosci*. 1993;13:2801–2820.
20. Sepulcre J, Liu H, Talukdar T, Martincorena I, Yeo BT, Buckner RL. The organization of local and distant functional connectivity in the human brain. *PLoS Comput Biol*. 2010;6:e1000808.
21. de Reus MA, van den Heuvel MP. The parcellation-based connectome: limitations and extensions. *Neuroimage*. 2013;80:397–404.
22. Chao-Gan Y, Yu-Feng Z. DPARSF: a MATLAB toolbox for "pipeline" data analysis of resting-state fMRI. *Front Syst Neurosci*. 2010;4:13.
23. Tzourio-Mazoyer N, Landeau B, Papathanassiou D, et al. Automated anatomical labeling of activations in SPM using a macroscopic anatomical parcellation of the MNI MRI single-subject brain. *Neuroimage*. 2002;15:273–289.
24. Watts DJ, Strogatz SH. Collective dynamics of 'small-world' networks. *Nature*. 1998;393:440–442.
25. Liao X, Vasilakos AV, He Y. Small-world human brain networks: perspectives and challenges. *Neurosci Biobehav Rev*. 2017;77:286–300.
26. Du H, Xia M, Zhao K, et al. PAGANI toolkit: parallel graph-theoretical analysis package for brain network big data. *Hum Brain Mapp*. 2018 doi: 10.1002/hbm.23996.
27. Wang Y, Du H, Xia M, et al. A hybrid CPU-GPU accelerated framework for fast mapping of high-resolution human brain connectome. *PLoS One*. 2013;8:e62789.
28. Du HX, Liao XH, Lin QX, et al. Test-retest reliability of graph metrics in high-resolution functional connectomics: a resting-state functional MRI study. *CNS Neurosci Ther*. 2015;21:802–816.
29. Liang X, Zou Q, He Y, Yang Y. Coupling of functional connectivity and regional cerebral blood flow reveals a physiological basis for network hubs of the human brain. *Proc Natl Acad Sci USA*. 2013;110:1929–1934.
30. Wang Y, Zhong S, Jia Y, et al. Disrupted resting-state functional connectivity in nonmedicated bipolar disorder. *Radiology*. 2016;280:529–536.
31. Argyelan M, Ikuta T, DeRosse P, et al. Resting-state fMRI connectivity impairment in schizophrenia and bipolar disorder. *Schizophr Bull*. 2014;40:100–110.
32. Skåtun KC, Kaufmann T, Tønnesen S, et al. Global brain connectivity alterations in patients with schizophrenia and bipolar spectrum disorders. *J Psychiatry Neurosci*. 2016;41:331–341.
33. Sheffield JM, Kandala S, Tamminga CA, et al. Transdiagnostic associations between functional brain network integrity and cognition. *JAMA Psychiatry*. 2017;74:605–613.
34. Rashid B, Arbabshirani MR, Damaraju E, et al. Classification of schizophrenia and bipolar patients using static and dynamic resting-state fMRI brain connectivity. *Neuroimage*. 2016;134:645–657.
35. Vargas C, López-Jaramillo C, Vieta E. A systematic literature review of resting state network–functional MRI in bipolar disorder. *J Affect Disord*. 2013;150:727–735.
36. Manelis A, Almeida JR, Stiffler R, Lockovich JC, Aslam HA, Phillips ML. Anticipation-related brain connectivity in bipolar and unipolar depression: a graph theory approach. *Brain*. 2016;139:2554–2566.
37. He H, Sui J, Du Y, et al. Co-altered functional networks and brain structure in unmedicated patients with bipolar and major depressive disorders. *Brain Struct Funct*. 2017;222:4051–4064.
38. Goya-Maldonado R, Brodmann K, Keil M, Trost S, Dechent P, Gruber O. Differentiating unipolar and bipolar depression by alterations in large-scale brain networks. *Hum Brain Mapp*. 2016;37:808–818.
39. Sharma A, Wolf DH, Ciric R, et al. Common dimensional reward deficits across mood and psychotic disorders: a connectome-wide association study. *Am J Psychiatry*. 2017;174:657–666.
40. Collin G, Scholtens LH, Kahn RS, Hillegers MHJ, van den Heuvel MP. Affected anatomical rich club and structural-functional coupling in young offspring of schizophrenia and bipolar disorder patients. *Biol Psychiatry*. 2017;82:746–755.

41. Stephan KE, Friston KJ, Frith CD. Dysconnection in schizophrenia: from abnormal synaptic plasticity to failures of self-monitoring. *Schizophr Bull*. 2009;35:509–527.
42. Lisman J. Low-frequency brain oscillations in schizophrenia. *JAMA Psychiatry*. 2016;73:298–299.
43. Moran LV, Hong LE. High vs low frequency neural oscillations in schizophrenia. *Schizophr Bull*. 2011;37:659–663.
44. Glausier JR, Lewis DA. Dendritic spine pathology in schizophrenia. *Neuroscience*. 2013;251:90–107.
45. Shen K, Hutchison RM, Bezgin G, Everling S, McIntosh AR. Network structure shapes spontaneous functional connectivity dynamics. *J Neurosci*. 2015;35:5579–5588.
46. Kolluri N, Sun Z, Sampson AR, Lewis DA. Lamina-specific reductions in dendritic spine density in the prefrontal cortex of subjects with schizophrenia. *Am J Psychiatry*. 2005;162:1200–1202.
47. Konopaske GT, Lange N, Coyle JT, Benes FM. Prefrontal cortical dendritic spine pathology in schizophrenia and bipolar disorder. *JAMA Psychiatry*. 2014;71:1323–1331.
48. Fiala JC, Spacek J, Harris KM. Dendritic spine pathology: cause or consequence of neurological disorders? *Brain Res Brain Res Rev*. 2002;39:29–54.
49. Blanpied TA, Ehlers MD. Microanatomy of dendritic spines: emerging principles of synaptic pathology in psychiatric and neurological disease. *Biol Psychiatry*. 2004;55:1121–1127.
50. Reichenberg A, Harvey PD, Bowie CR, et al. Neuropsychological function and dysfunction in schizophrenia and psychotic affective disorders. *Schizophr Bull*. 2009;35:1022–1029.
51. Velthorst E, Fett AJ, Reichenberg A, et al. The 20-year longitudinal trajectories of social functioning in individuals with psychotic disorders. *Am J Psychiatry*. 2017;174:1075–1085.
52. Ingvar DH, Franzén G. Abnormalities of cerebral blood flow distribution in patients with chronic schizophrenia. *Acta Psychiatr Scand*. 1974;50:425–462.
53. Ragland JD, Yoon J, Minzenberg MJ, Carter CS. Neuroimaging of cognitive disability in schizophrenia: search for a pathophysiological mechanism. *Int Rev Psychiatry*. 2007;19:417–427.
54. Ragland JD, Gur RC, Glahn DC, et al. Frontotemporal cerebral blood flow change during executive and declarative memory tasks in schizophrenia: a positron emission tomography study. *Neuropsychology*. 1998;12:399–413.
55. Potkin SG, Turner JA, Brown GG, et al.; FBIRN. Working memory and DLPFC inefficiency in schizophrenia: the FBIRN study. *Schizophr Bull*. 2009;35:19–31.
56. Callicott JH, Mattay VS, Verchinski BA, Marenco S, Egan MF, Weinberger DR. Complexity of prefrontal cortical dysfunction in schizophrenia: more than up or down. *Am J Psychiatry*. 2003;160:2209–2215.
57. Gur RC, Gur RE. Hypofrontality in schizophrenia: RIP. *Lancet*. 1995;345:1383–1384.
58. Walter H, Wunderlich AP, Blankenhorn M, et al. No hypofrontality, but absence of prefrontal lateralization comparing verbal and spatial working memory in schizophrenia. *Schizophr Res*. 2003;61:175–184.
59. Sheppard G, Gruzelier J, Manchanda R, et al. 15O positron emission tomographic scanning in predominantly never-treated acute schizophrenic patients. *Lancet*. 1983;2:1448–1452.
60. Meda SA, Wang Z, Ivleva EI, et al. Frequency-specific neural signatures of spontaneous low-frequency resting state fluctuations in psychosis: evidence from bipolar-schizophrenia network on intermediate phenotypes (B-SNIP) consortium. *Schizophr Bull*. 2015;41:1336–1348.
61. Turner JA, Damaraju E, van Erp TG, et al. A multi-site resting state fMRI study on the amplitude of low frequency fluctuations in schizophrenia. *Front Neurosci*. 2013;7:137.
62. Yu R, Chien YL, Wang HL, et al. Frequency-specific alternations in the amplitude of low-frequency fluctuations in schizophrenia. *Hum Brain Mapp*. 2014;35:627–637.
63. Button KS, Ioannidis JP, Mokrysz C, et al. Power failure: why small sample size undermines the reliability of neuroscience. *Nat Rev Neurosci*. 2013;14:365–376.
64. Friston KJ. Functional and effective connectivity: a review. *Brain Connect*. 2011;1:13–36.
65. Wang S, Zhan Y, Zhang Y, et al. Abnormal long- and short-range functional connectivity in adolescent-onset schizophrenia patients: a resting-state fMRI study. *Prog Neuropsychopharmacol Biol Psychiatry*. 2018;81:445–451.
66. Wang Y, Tang W, Fan X, et al. Resting-state functional connectivity changes within the default mode network and the salience network after antipsychotic treatment in early-phase schizophrenia. *Neuropsychiatr Dis Treat*. 2017;13:397–406.
67. Houck JM, Çetin MS, Mayer AR, et al. Magnetoencephalographic and functional MRI connectomics in schizophrenia via intra- and inter-network connectivity. *Neuroimage*. 2017;145:96–106.
68. Katz G, Rangel-Eudave G, Allen-Leigh B, Lazcano-Ponce E. A best practice in education and support services for independent living of intellectually disabled youth and adults in Mexico. *Salud Publica Mex*. 2008;50(suppl 2):s194–s204.
69. Tagliazucchi E, Laufs H. Decoding wakefulness levels from typical fMRI resting-state data reveals reliable drifts between wakefulness and sleep. *Neuron*. 2014;82:695–708.
70. Horovitz SG, Braun AR, Carr WS, et al. Decoupling of the brain's default mode network during deep sleep. *Proc Natl Acad Sci USA*. 2009;106:11376–11381.
71. Larson-Prior LJ, Zempel JM, Nolan TS, Prior FW, Snyder AZ, Raichle ME. Cortical network functional connectivity in the descent to sleep. *Proc Natl Acad Sci USA*. 2009;106:4489–4494.
72. Logothetis NK. What we can do and what we cannot do with fMRI. *Nature*. 2008;453:869–878.
73. Florin E, Watanabe M, Logothetis NK. The role of sub-second neural events in spontaneous brain activity. *Curr Opin Neurobiol*. 2015;32:24–30.
74. Lichtman JW, Pfister H, Shavit N. The big data challenges of connectomics. *Nat Neurosci*. 2014;17:1448–1454.
75. Scholtens LH, Schmidt R, de Reus MA, van den Heuvel MP. Linking macroscale graph analytical organization to microscale neuroarchitectonics in the macaque connectome. *J Neurosci*. 2014;34:12192–12205.
76. Schroeter MS, Charlesworth P, Kitzbichler MG, Paulsen O, Bullmore ET. Emergence of rich-club topology and coordinated dynamics in development of hippocampal functional networks in vitro. *J Neurosci*. 2015;35:5459–5470.
77. Shimono M, Beggs JM. Functional clusters, hubs, and communities in the cortical microconnectome. *Cereb Cortex*. 2015;25:3743–3757.
78. Hagmann P, Cammoun L, Gigandet X, et al. Mapping the structural core of human cerebral cortex. *PLoS Biol*. 2008;6:e159.
79. Honey CJ, Sporns O, Cammoun L, et al. Predicting human resting-state functional connectivity from structural connectivity. *Proc Natl Acad Sci USA*. 2009;106:2035–2040.

80. Alexander-Bloch A, Raznahan A, Bullmore E, Giedd J. The convergence of maturational change and structural covariance in human cortical networks. *J Neurosci*. 2013;33:2889–2899.
81. Wang Z, Dai Z, Gong G, Zhou C, He Y. Understanding structural-functional relationships in the human brain: a large-scale network perspective. *Neuroscientist*. 2015;21:290–305.
82. Sporns O, Kötter R. Motifs in brain networks. *PLoS Biol*. 2004;2:e369.
83. Goñi J, van den Heuvel MP, Avena-Koenigsberger A, et al. Resting-brain functional connectivity predicted by analytic measures of network communication. *Proc Natl Acad Sci USA*. 2014;111:833–838.
84. Vértes PE, Alexander-Bloch AF, Gogtay N, Giedd JN, Rapoport JL, Bullmore ET. Simple models of human brain functional networks. *Proc Natl Acad Sci USA*. 2012;109:5868–5873.
85. Power JD, Barnes KA, Snyder AZ, Schlaggar BL, Petersen SE. Spurious but systematic correlations in functional connectivity MRI networks arise from subject motion. *Neuroimage*. 2012;59:2142–2154.
86. Van Dijk KR, Sabuncu MR, Buckner RL. The influence of head motion on intrinsic functional connectivity MRI. *Neuroimage*. 2012;59:431–438.
87. Zeng LL, Wang D, Fox MD, et al. Neurobiological basis of head motion in brain imaging. *Proc Natl Acad Sci USA*. 2014;111:6058–6062.
88. Couvy-Duchesne B, Blokland GA, Hickie IB, et al. Heritability of head motion during resting state functional MRI in 462 healthy twins. *Neuroimage*. 2014;102 Pt 2:424–434.
89. Engelhardt LE, Roe MA, Juranek J, et al. Children's head motion during fMRI tasks is heritable and stable over time. *Dev Cogn Neurosci*. 2017;25:58–68.
90. Kong XZ, Zhen Z, Li X, et al. Individual differences in impulsivity predict head motion during magnetic resonance imaging. *PLoS One*. 2014;9:e104989.
91. Mueller S, Wang D, Fox MD, et al. Individual variability in functional connectivity architecture of the human brain. *Neuron*. 2013;77:586–595.
92. Finn ES, Shen X, Scheinost D, et al. Functional connectome fingerprinting: identifying individuals using patterns of brain connectivity. *Nat Neurosci*. 2015;18:1664–1671.
93. Liu J, Liao X, Xia M, He Y. Chronnectome fingerprinting: identifying individuals and predicting higher cognitive functions using dynamic brain connectivity patterns. *Hum Brain Mapp*. 2018;39:902–915.
94. Drysdale AT, Grosenick L, Downar J, et al. Resting-state connectivity biomarkers define neurophysiological subtypes of depression. *Nat Med*. 2017;23:28–38.
95. Insel TR, Cuthbert BN. Medicine. Brain disorders? Precisely. *Science*. 2015;348:499–500.
96. Xia M, He Y. Functional connectomics from a "big data" perspective. *Neuroimage*. 2017;160:152–167.
97. Xia M, Wang J, He Y. BrainNet Viewer: a network visualization tool for human brain connectomics. *PLoS One*. 2013;8:e68910.